Supporting Information

Grain Boundary and Misorientation Angle Dependent Thermal Transport in Single-layer MoS_2

Ke Xu,[1] Ting Liang,[2] Zhisen Zhang,[1] Xuezheng Cao,[1] Meng Han,[2] Ning Wei [3,*] and Jianyang Wu[1, 4,*]

[1]Department of Physics, Research Institute for Biomimetics and Soft Matter, Jiujiang Research Institute and Fujian Provincial Key Laboratory for Soft Functional Materials Research, Xiamen University, Xiamen 361005, PR China

[2]Shenzhen Institute of Advanced Electronic Materials, Shenzhen Institute of Advanced Technology, Chinese Academy of Sciences, Shenzhen 518055, China

[3]Jiangsu Key Laboratory of Advanced Food Manufacturing Equipment and Technology, Jiangnan University, 214122, Wuxi, China

[4]NTNU Nanomechanical Lab, Norwegian University of Science and Technology (NTNU), Trondheim 7491, Norway

[*] Corresponding authors: weining@mail.tsinghua.edu.cn; jianyang@xmu.edu.cn

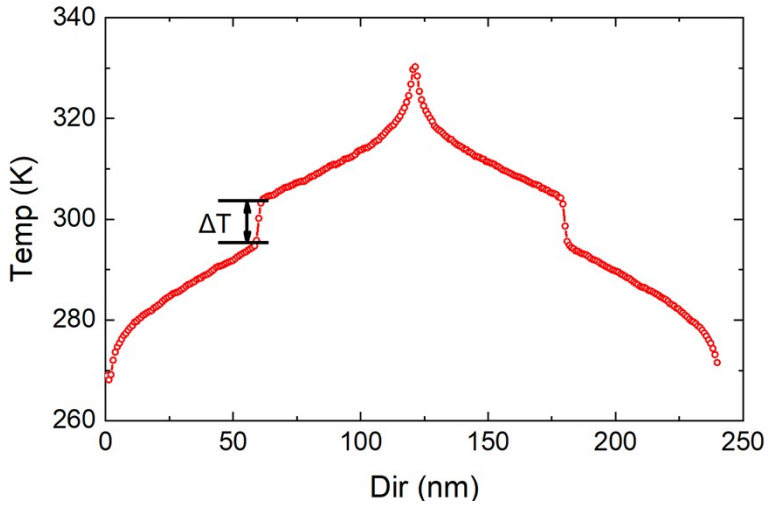

Figure S1 Typical temperature distribution profiles perpendicular to the GBs predicted from RNEMD simulations

Table S1 The GB tilt angle θ, Kapitza resistance R, grain boundary line tension γ, and defect density ρ for the GB $SLMoS_2$ samples considered here

Armchair-oriented GBs						Zigzag-oriented GBs			
Mo5|7 GBs				S5|7 GBs					
θ (°)	ρ 1/nm	R $m^2 \cdot K \cdot GW^{-1}$	γ eV/nm	R $m^2 \cdot KW^{-1}$	γ eV/nm	θ (°)	R $m^2 \cdot K \cdot GW^{-1}$	ρ 1/nm	γ eV/nm
21.98	1.19	1.24	6.62	1.40	4.23	31.78	2.51	1.77	6.50
18.82	1.00	1.05	6.31	1.17	4.26	38.05	1.66	1.37	6.05
17.96	0.97	1.06	6.12	0.96	4.17	42.03	1.20	1.13	5.72
16.46	0.90	0.85	5.79	0.92	4.00	44.78	1.04	0.96	5.37
13.16	0.72	0.73	4.89	0.84	3.47	46.80	0.91	0.83	5.08
9.40	0.52	0.53	3.93	0.68	2.90	48.35	0.88	0.74	4.89
7.31	0.37	0.43	3.32	0.54	2.52	49.57	0.80	0.66	4.66
5.98	0.33	0.32	2.89	0.36	2.23	51.38	0.65	0.55	4.26
5.06	0.26	0.24	2.49	0.29	2.00	52.65	0.45	0.47	3.86

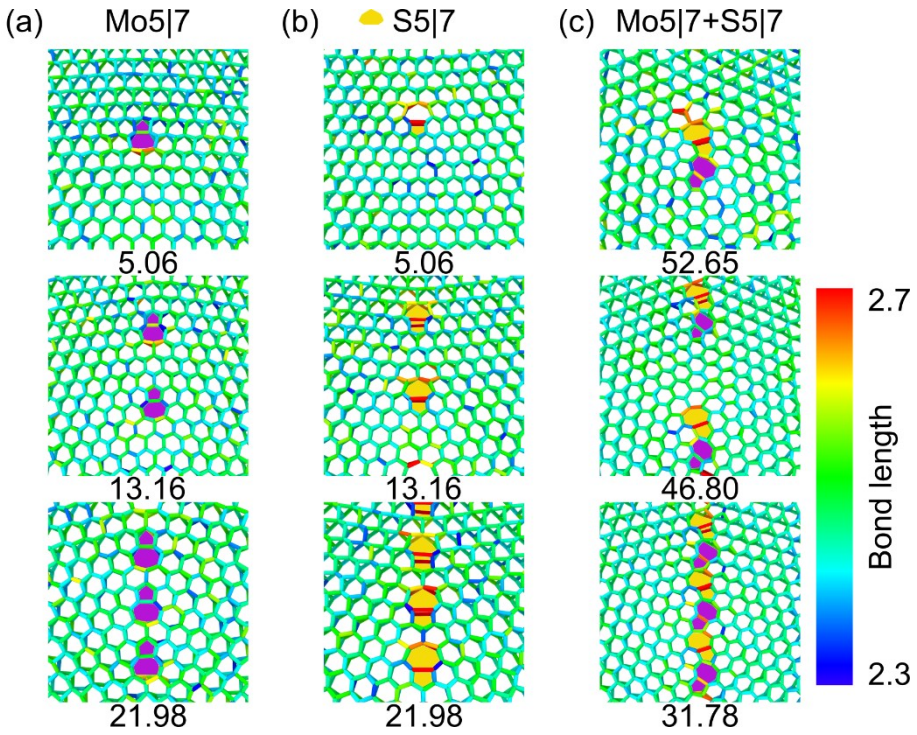

Figure S2 Deformation of bond configuration at GB regions. (a)-(c) Contours of bond length of Mo5|7, S5|7 and Mo5|7+S5|7 dislocation-dominated GBs with three different misorientation angles (θ), respectively.zz

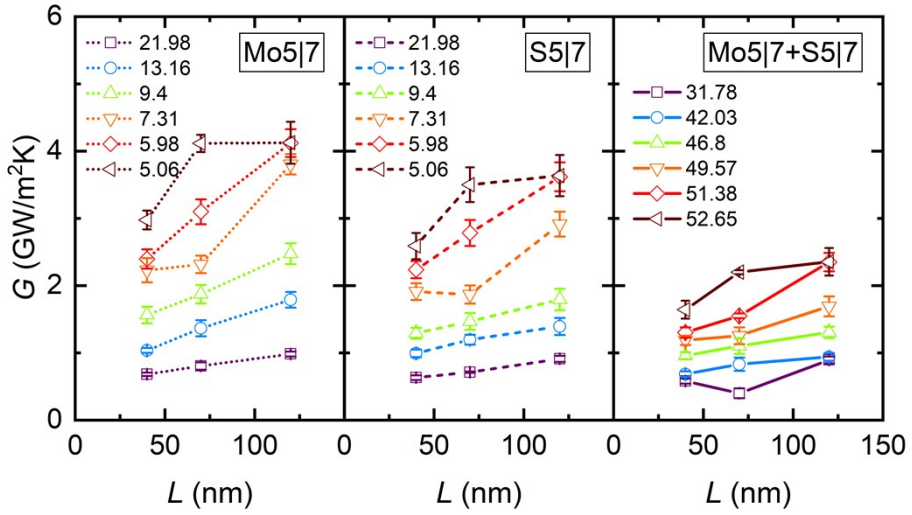

Figure S3 Thermal conductance G as a function of the length of crystalline grains of bicrystals with different misorientation angle of GBs. The dot/solid/dashed line indicates the Mo5|7/S5|7/Mo5|7+S5|7 -oriented GBs.

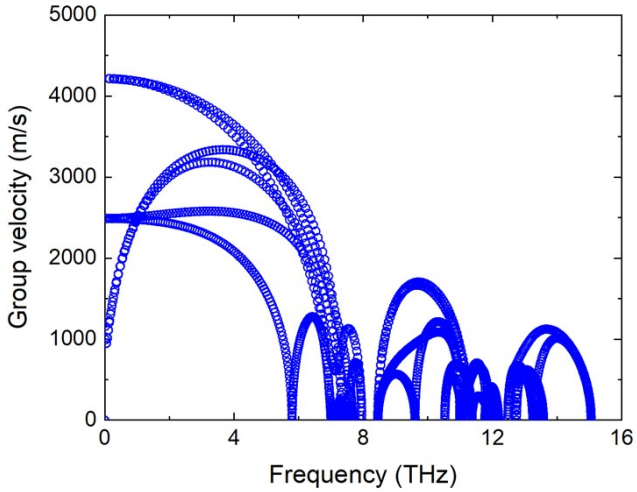

Figure S4 Phonon group velocity of pristine single-layer MoS_2

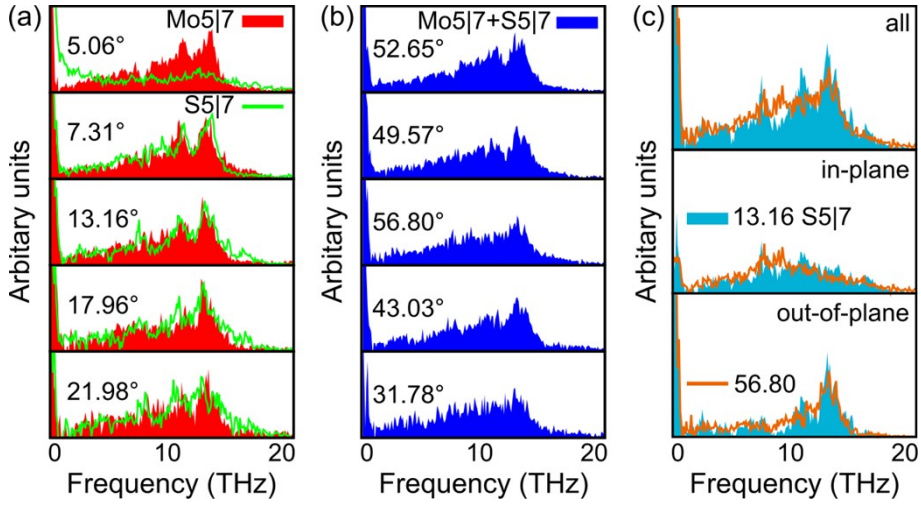

Figure S5 Phonon vibrational density of state (*v*DOS) of single-layer MoS_2 bicrystals. (a) and (c) *v*DOS of Mo5|7 and Mo5|7+S5|7 dislocation-dominated MoS_2 bicrystals with five different misorientation angles (θ), respectively. (b) and (d) Comparison of total, in-plane and out-of-plane *v*DOS of MoS_2 bicrystals between Mo5|7 and S5|7, Mo5|7 and Mo5|7+S5|7 dislocation-dominated GBs, respectively.

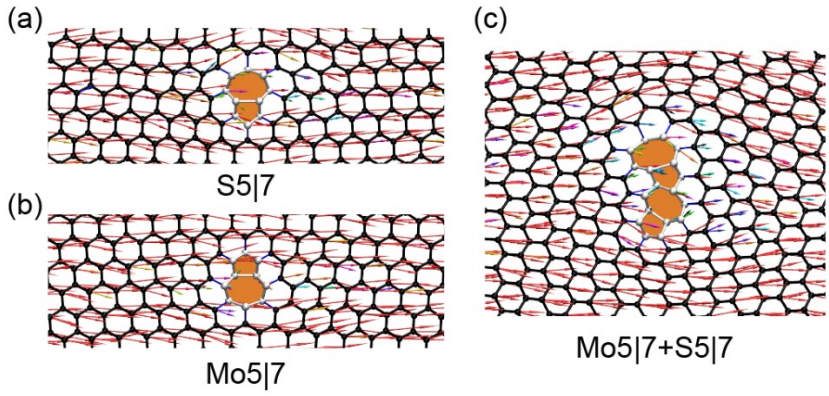

Figure S6 Microscopic heat flux by vectors in 5|7 dislocation-contained $SLMoS_2$